



Dynamic responses of the adrenal steroidogenic regulatory network

Francesca Spiga^{a,1,2}, Eder Zavala^{b,c,d,1}, Jamie J. Walker^{a,c,d,e,1}, Zidong Zhao^a, John R. Terry^{b,c,d}, and Stafford L. Lightman^{a,d}

^aHenry Wellcome Laboratories for Integrative Neuroscience and Endocrinology, University of Bristol, Bristol BS1 3NY, United Kingdom; ^bLiving Systems Institute, University of Exeter, Exeter EX4 4QD, United Kingdom; ^cWellcome Trust Centre for Biomedical Modelling and Analysis, University of Exeter, Exeter EX4 4QD, United Kingdom; ^dEPSRC Centre for Predictive Modelling in Healthcare, University of Exeter, Exeter EX4 4QD, United Kingdom; and ^eCollege of Engineering, Mathematics and Physical Sciences, University of Exeter, Exeter EX4 4QF, United Kingdom

Edited by Bruce S. McEwen, The Rockefeller University, New York, NY, and approved June 22, 2017 (received for review March 8, 2017)

The hypothalamic–pituitary–adrenal axis is a dynamic system regulating glucocorticoid hormone synthesis in the adrenal glands. Many key factors within the adrenal steroidogenic pathway have been identified and studied, but little is known about how these factors function collectively as a dynamic network of interacting components. To investigate this, we developed a mathematical model of the adrenal steroidogenic regulatory network that accounts for key regulatory processes occurring at different timescales. We used our model to predict the time evolution of steroidogenesis in response to physiological adrenocorticotrophic hormone (ACTH) perturbations, ranging from basal pulses to larger stress-like stimulations (e.g., inflammatory stress). Testing these predictions experimentally in the rat, our results show that the steroidogenic regulatory network architecture is sufficient to respond to both small and large ACTH perturbations, but coupling this regulatory network with the immune pathway is necessary to explain the dissociated dynamics between ACTH and glucocorticoids observed under conditions of inflammatory stress.

adrenal gland | glucocorticoids | steroidogenesis | stress response | mathematical modeling

The hypothalamic–pituitary–adrenal (HPA) axis is a stress-responsive neuroendocrine system that controls circulating levels of the vital glucocorticoid (CORT) hormones corticosterone (in rodents) and cortisol (in humans). These are steroids synthesized by the adrenal gland in response to stimulation by adrenocorticotrophic hormone (ACTH), which is secreted by the anterior pituitary in response to corticotrophin-releasing hormone (CRH) and arginine vasopressin released from hypothalamic paraventricular neurons. These neurons receive circadian inputs from the suprachiasmatic nucleus and are activated in response to stress. Via the bloodstream, CORT accesses target tissues where it mediates metabolic, cognitive, and immune responses. CORT also regulates its own production through negative feedback inhibition of ACTH and CRH secretion from the pituitary and hypothalamus, respectively. To mount an effective response to stress, CORT must be secreted rapidly by the adrenal glands. However, because of its lipophilic nature, CORT cannot be prestored in vesicles and must therefore be rapidly synthesized *de novo* in response to ACTH stimulation.

Under basal, unstressed conditions, ACTH and CORT exhibit ultradian oscillations. Although there is some evidence for pulsatility of CRH (1, 2), our recent work suggests that ACTH and CORT pulsatility is predominantly generated by a subhypothalamic oscillator within the pituitary–adrenal system (3, 4). The amplitude of these pulses varies in a circadian manner with larger pulses occurring at the start of the active phase (morning in humans, evening in rodents). Under normal physiological conditions, CORT secretion is tightly correlated with ACTH (5). However, there are a number of conditions where a dynamic dissociation between these hormones occurs (reviewed in ref. 6). For example, there is evidence that proinflammatory cytokines released during inflammation can potentiate adrenal responsiveness to ACTH and can activate the adrenal steroidogenic pathway directly (7). Recent examples of

this are the hormonal stress responses observed during cardiac surgery in humans and in a rodent model of inflammation (8). It has been hypothesized that this dynamic dissociation is due to increased adrenal sensitivity to ACTH, presumably as a result of the effect of circulating proinflammatory cytokines. Thus, a better understanding of the mechanisms that regulate steroidogenesis is necessary to explain the dynamic response of CORT to both physiological and pathological ACTH perturbations.

Within cells of the adrenal cortex zona fasciculata, steroidogenesis is regulated by several processes operating over a range of timescales: there are rapid nongenomic processes, as well as slower processes that depend on gene expression. Together, these form a complex pathway that is activated when ACTH binds the melanocortin type-2 receptor (MC2R), resulting in rapid phosphorylation of proteins involved in cholesterol metabolism—the substrate for CORT synthesis. These include hormone-sensitive lipase (HSL) and steroidogenic acute regulatory (StAR) proteins, which control levels of intracellular cholesterol and its transport within the mitochondrial matrix, respectively (9, 10). In addition to these rapid, nongenomic events, ACTH simultaneously triggers a slower genomic response involving the expression of steroidogenic genes such as *StAR*, *CYP11A*, *MC2R*, and *MRAP*. These genes are transcriptionally regulated by a number of nuclear receptors, the activity and expression of which are also under the control of ACTH. Specifically, ACTH induces the “positive regulators” steroidogenic factor 1 (SF-1) (11) and Nur77 (NR4A1) (12) and inhibits the “negative regulator” DAX-1 (dosage sensitive sex-reversal, adrenal hypoplasia

Significance

Our ability to respond to stress depends on a remarkably dynamic process of hormone secretion. The rapid release of glucocorticoid hormones from the adrenal glands is critical to mount such an efficient response to stress, particularly during inflammation. Although many key factors involved in this process have been studied, the way in which these factors interact dynamically with one another to regulate glucocorticoid secretion has not been investigated. Here, we develop a mathematical model of the regulatory network controlling glucocorticoid synthesis and, by combining this with *in vivo* experiments, show how this network governs changes in adrenal responsiveness under basal unstressed physiological conditions and under exposure to inflammatory stress.

Author contributions: F.S., J.J.W., J.R.T., and S.L.L. designed research; F.S. and Z.Z. performed experiments; F.S., E.Z., and J.J.W. analyzed data; E.Z. and J.J.W. developed and analyzed mathematical models; F.S., E.Z., and J.J.W. wrote the paper with revision by all authors.

The authors declare no conflict of interest.

This article is a PNAS Direct Submission.

Freely available online through the PNAS open access option.

¹F.S., E.Z., and J.J.W. contributed equally to this work.

²To whom correspondence should be addressed. Email: f.spiga@bristol.ac.uk.

This article contains supporting information online at www.pnas.org/lookup/suppl/doi:10.1073/pnas.1703779114/-DCSupplemental.

congenita locus on the X chromosome) (13). These interacting cascades of genomic and nongenomic events work in combination to activate and maintain optimal levels of steroidogenic proteins, ultimately leading to mitochondrial import of cholesterol and CORT synthesis. In addition, our recent mathematical modeling of the CORT response to ACTH suggests that a rapid, intra-adrenal CORT negative feedback loop constitutes an additional control mechanism of steroidogenesis (14–17). The biological processes underlying this self-inhibition are not known, but the glucocorticoid receptor (GR) is expressed in the adrenal cortex (15, 18). Furthermore, the synthetic glucocorticoid dexamethasone—a specific GR agonist—has been shown to inhibit ACTH-induced corticosterone secretion from rat adrenocortical cells (19) as well as the transcription of steroidogenic genes through a mechanism that involves GR- and SF-1-mediated induction of DAX-1 expression (20).

Although many of the components involved in the steroidogenic pathway have been identified, it remains unclear how their mutual interaction regulates CORT dynamics. In this study, we considered the core components of the steroidogenic regulatory network (SRN) and investigated how the cross-talk among these components underlies ACTH-responsive CORT dynamics. To understand the time evolution of steroidogenesis following ACTH stimulation, we developed a mathematical model of the SRN based on the complex molecular interactions within the SRN, including the intra-adrenal GR-CORT connection that feeds back on the genomic pathway. We used this model to characterize dynamic responses to a variety of perturbations and to make predictions that we then tested experimentally. Our results show that it is the complex interactions between components of the SRN that govern dynamic steroidogenic responses in adrenocortical cells. Importantly, the SRN architecture enables cells to respond to both small and large ACTH perturbations, but is not sufficient to explain the dynamic response to inflammatory stress; in this case, we found that the CORT response can only be explained by coupling the SRN with the immune pathway. This work provides a theoretical framework to study adrenal CORT responses to a range of physiological and pathological perturbations, building upon our previous work on the

role of glucocorticoid-mediated negative feedback loops regulating the ultradian dynamics of the HPA axis (3, 4).

Results

A Short Pulse of ACTH Dynamically Activates the SRN. To explore systematically how dynamic responses result from complex interactions within the SRN, we developed a mathematical model of the regulatory network. To aid analysis, we restrained the complexity of the model by stripping off nonessential regulatory components from the network architecture. This was performed by including only those nodes within the SRN that have been shown to be involved in CORT-mediated feedback loops and participate in cross-talk with StAR (Fig. 1; see *SI Appendix, Fig. S1* for the full SRN) (20–25). Specifically, the model consists of a set of delay differential equations (DDEs) that describe the dynamics of intra-adrenal levels of CORT (A-CORT) and phosphorylation of GR (pGR, a marker of GR activation), and the expression of DAX-1, SF-1 and StAR following “virtual” (in silico) stimulation by ACTH (*SI Appendix, Fig. S2* and *Mathematical Model*).

To assist the calibration of our mathematical model, we first considered the response of the SRN to a single pulse of ACTH, which is similar to an endogenous ultradian pulse of ACTH (Fig. 2A). To do this, we performed an in vivo experiment in the rat to characterize the dynamic response of the adrenal SRN to an i.v. injection of ACTH. We measured steroidogenic factors in the core SRN (Fig. 1), as well as some additional factors that are also involved in steroidogenesis but were not considered in the model. The i.v. ACTH injection resulted in a rapid and transient increase in plasma ACTH (Fig. 2A) with a peak concentration comparable to the peak of endogenous ultradian ACTH pulses (26, 27). This was accompanied by a rapid and dynamic increase in CORT secretion, detectable in both adrenal tissue (A-CORT; Fig. 2B) and blood plasma (P-CORT; *SI Appendix, Fig. S3B*). To assess the dynamics of GR activation following the i.v. ACTH injection, we measured pGR at Serine 211 (28). pGR demonstrated a rapid, significant increase (Fig. 2C), and its pattern of activation was similar to the observed pattern of A-CORT (Fig. 2B).

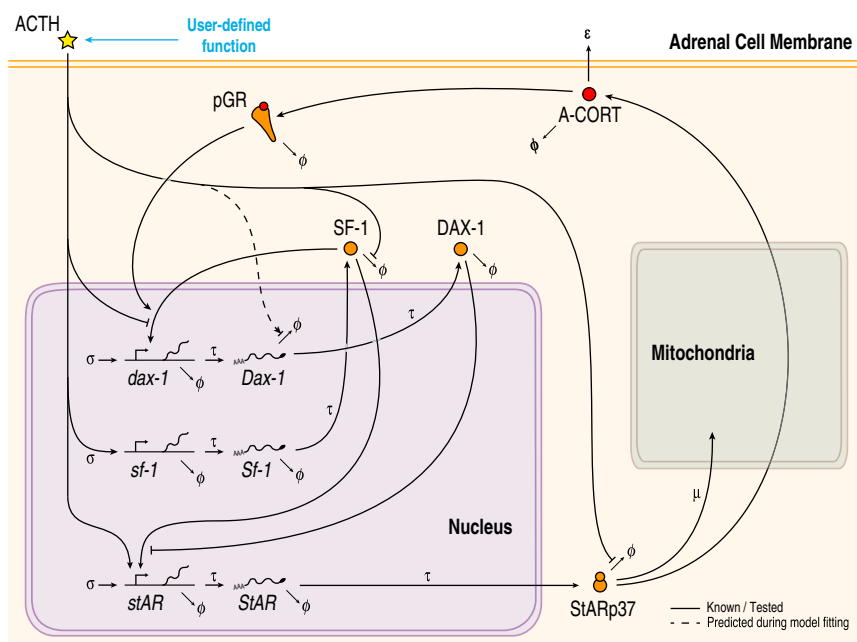


Fig. 1. The simplified SRN represented in the mathematical model accounts for both genomic and nongenomic processes occurring at different time scales. Also considered in the model are the A-CORT/GR-mediated intra-adrenal feedback loop and posttranscriptional and posttranslational processes, including the ACTH-mediated stabilization of StARp37.

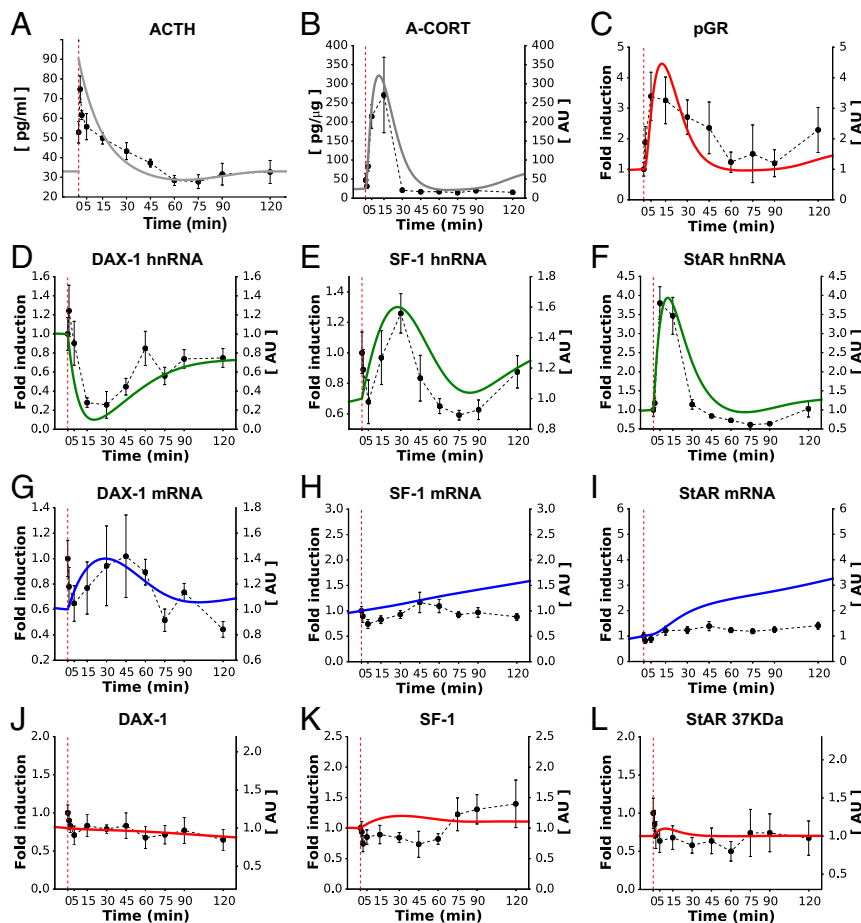


Fig. 2. The calibrated model reproduced the SRN dynamics following a short pulse of ACTH (A). Fitting the model to data successfully reproduced the rapid and transient synthesis of A-CORT (B) and GR activation (C). The model also made qualitative predictions about the induction of DAX-1, SF-1, and StAR genes (D–F) that closely matched the *in vivo* data. Similarly, the model approximated the expression of the gene products, as judged from the dynamics of mRNA (G–I) and protein levels (J–L). Red dashed lines indicate the time of ACTH injection. Representative Western immunoblotting images for pGR, StARp37, SF-1, and DAX-1 are shown in *SI Appendix, Fig. S3*.

ACTH also regulates steroidogenesis over a slightly slower time frame via modulation of the expression of genes involved in CORT synthesis. We therefore determined the effects of the *i.v.* ACTH injection on the dynamic expression of key steroidogenic genes in the adrenal SRN. Because many ACTH-regulated genes require activation of CREB to be transcribed, we first assessed the dynamics of CREB phosphorylation (pCREB). Consistent with previous reports (29, 30), there was a rapid and transient increase in pCREB (*SI Appendix, Fig. S3D*). We then investigated the dynamic transcription of steroidogenic genes by measuring their heteronuclear RNA (hnRNA) and mRNA levels. As expected, the dynamics of pCREB were paralleled by a transient activation of StAR hnRNA, followed by a slower StAR mRNA accumulation (Fig. 2 F and I). In response to the *i.v.* ACTH injection, there was a rapid, transient decrease in DAX-1 hnRNA and a dynamic increase in SF-1 hnRNA (Fig. 2 D and E). In contrast, no significant changes in DAX-1 and SF-1 mRNA (Fig. 2 G and H), and in DAX-1, SF-1, and StARp37 protein levels were detected within 2 h of ACTH administration (Fig. 2 J–L).

With respect to those SRN factors that were not considered in the model, we found that the *i.v.* ACTH injection also had a rapid effect on the activity of HSL, a protein that plays a key role in the SRN by regulating intracellular metabolism of cholesterol (*SI Appendix, Fig. S3C*). We assessed this by measuring the phosphorylation dynamics at sites known to increase HSL activity (pHSL at Serine 660 and 563) (31) and observed a dynamic

activation of both pHSL-(Ser660) and pHSL-(Ser563). The pHSL dynamics suggest that a rapid, transient increase in intracellular free cholesterol precedes CORT synthesis and supports previous findings that phosphorylation of HSL is a crucial step in the steroidogenic process. Furthermore, ACTH rapidly activated hnRNA and mRNA levels of MC2R, MRAP, Nur77, and CYP11A1, but had no effect on HSL hnRNA and mRNA (*SI Appendix, Fig. S3E*). No significant changes in CYP11A1, StARp32, StARp30, or HSL protein levels were detected within 2 h of ACTH administration (*SI Appendix, Fig. S3F*). Taken together, these results show that dynamic changes within both nongenomic and genomic processes are involved in the dynamic regulation of steroidogenesis.

Next, we fitted the model to the experimental data (Fig. 2). In addition to recalibrating model parameters, we further considered a potential posttranscriptional regulatory mechanism: an ACTH dose-dependent control of DAX-1 mRNA stability that accounts for the DAX-1 mRNA levels of varying magnitude observed following ACTH stimuli (32) (*SI Appendix, Mathematical Model and Fig. S4*). The time evolution of the SRN was generated by driving the mathematical model with a virtual ACTH pulse given during the nadir of the circadian rhythm (*SI Appendix, Fig. S2 and Mathematical Model*). These simulations showed that the A-CORT dynamics exhibited a rising phase at <5 min, a peak at ~10 min, and a falling phase at >15 min (Fig. 2B). Similarly, the pGR dynamics predicted by the model displayed a rising phase at <5 min,

a peak phase at ~ 12 min, and a falling phase at >15 min (Fig. 2C). The model also predicted a transient induction of the SF-1 and StAR genes, as judged from their rapidly inducible primary transcripts (hnRNA), mRNA, and protein dynamics (Fig. 2 E, F, H, I, K, and L). In contrast, the model predicted a transient inhibition of DAX-1 hnRNA, but a transient induction of its mRNA and protein levels (Fig. 2 D, G, and J). Taken together, these simulations closely matched the *in vivo* data for A-CORT and pGR dynamics, as well as gene induction (Fig. 2 B–F). Although the changes in mRNA and protein levels measured *in vivo* were not statistically significant, our model still reproduced the transient dynamics of DAX-1 mRNA and protein (Fig. 2 G and J) and predicted a gradual increase of SF-1 and StAR mRNA and protein (Fig. 2 H, I, K, and L) that is consistent with the transient increase of their corresponding hnRNAs. Discrepancies between the model and experimental data may originate from unexplored posttranscriptional or posttranslational regulatory mechanisms of SF-1 and StAR expression that the model does not account for.

Dynamic Responses of the SRN to Large ACTH Perturbations. Our data above show that an ACTH stimulus comparable to an endogenous ultradian pulse leads to dynamic changes within the SRN, ultimately driving the tightly correlated dynamic release of CORT. However, the adrenal gland is also subjected to more forceful perturbations (e.g., those associated with acute stressors), and in some cases the tight correlation between ACTH and

CORT is lost. This “dissociation” has been implicated in a change of the adrenal’s sensitivity to ACTH (reviewed in ref. 6), suggesting that the SRN has the ability to decode ACTH signals in a context-dependent manner. Motivated by this, we used our model to investigate how the SRN responds to a larger ACTH perturbation, comparable to that measured in response to an inflammatory stress (8), and tested our model predictions experimentally.

We have previously developed an experimental methodology to apply a large ACTH stimulus to the rat adrenal glands (8). This consists of four sequential *s.c.* injections of ACTH at 35-min intervals, which results in a large surge in ACTH plasma concentrations comparable to that observed during inflammatory stress (Fig. 3A). To explore how such a substantial ACTH perturbation affects the dynamics of components within the adrenal SRN, we drove our model with this same pattern of ACTH stimulation and simulated the transient dynamics of CORT and pGR, as well as DAX-1, SF-1, and StAR. Our model predicted a rapid, transient increase in A-CORT consisting of a rising phase (<30 min), a plateau (45–120 min), and a falling phase (>120 min) (Fig. 3B). As expected, the pGR dynamic profile predicted by the model was consistent with that of A-CORT (Fig. 3C). In terms of gene expression, the model predicted a transient inhibition of DAX-1 gene expression, as well as a transient induction of SF-1 and StAR genes (Fig. 3 D–J). Regarding protein levels, our model produced a transient activation of SF-1 and StARp37 and a gradual decline in DAX-1 (Fig. 3 J–L).

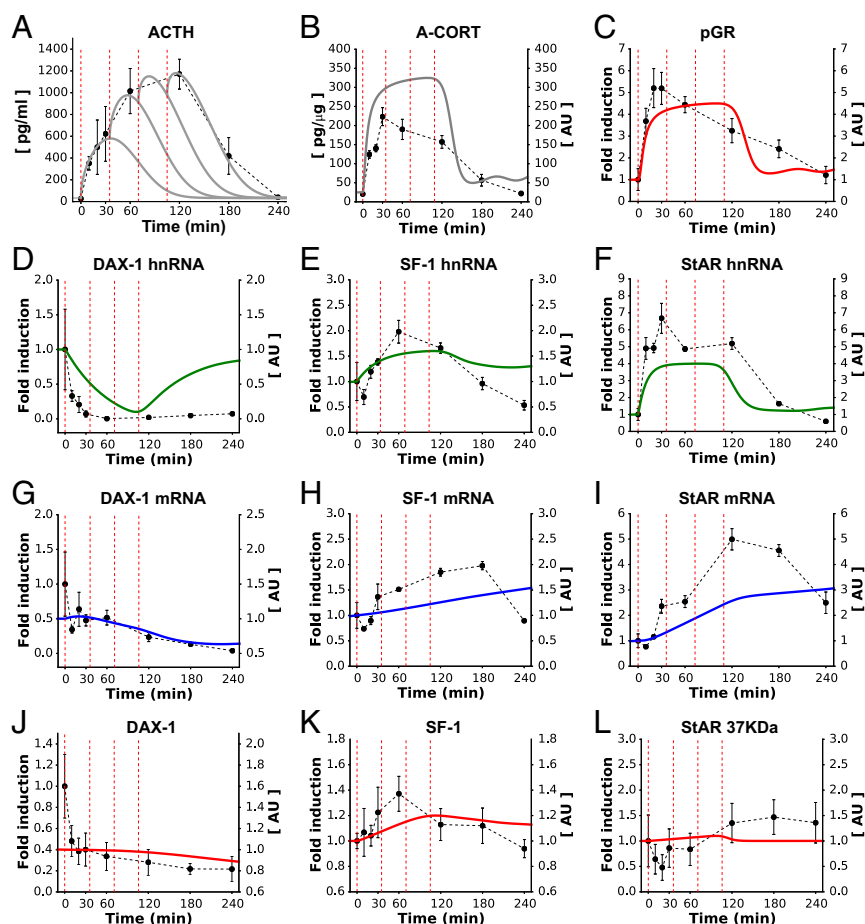


Fig. 3. The model reproduced the SRN dynamics following a high dose of ACTH (A). The model successfully reproduced the long and transient surges of A-CORT (B) and GR activation (C) and also made qualitative predictions about the induction of DAX-1, SF-1, and StAR genes (D–F) that closely matched the *in vivo* data. Similarly, the model approximated the expression of the gene products, as judged from the dynamics of mRNA (G–I) and protein levels (J–L). Red dashed lines indicate the time of ACTH injections. Representative Western immunoblotting images for pGR, StARp37, SF-1, and DAX-1 are shown in *SI Appendix, Fig. S5*.

To test these modeling predictions, we measured the dynamic response of the rat SRN to this ACTH challenge. The increase in plasma ACTH levels was paralleled by a robust increase in both A-CORT (Fig. 3B) and P-CORT (*SI Appendix, Fig. S5B*). As observed in the i.v. ACTH pulse experiment, there was a dynamic increase in pGR that was consistent with the observed pattern of A-CORT (Fig. 3C). Consistent with the ACTH i.v. pulse data, there was a significant decrease in DAX-1 hnRNA and mRNA (Fig. 3D and G) and a significant increase in SF-1 and StAR hnRNA and mRNA (Fig. 3E, F, H, and I). With regard to protein levels, the high dose of ACTH also induced a significant increase in StArp30 (*SI Appendix, Fig. S5F*), but not in StArp37 (Fig. 3L), StArp32 (*SI Appendix, Fig. S5F*), or SF-1 (Fig. 3K). There was a nonsignificant decrease in DAX-1 protein (Fig. 3J). The dynamic effects of a high dose of ACTH on A-CORT were paralleled by an increase in both pHSL-(Ser660) and pHSL-(Ser563) (*SI Appendix, Fig. S5C*). Furthermore, dynamic transcription of StAR was accompanied by dynamic changes in pCREB (*SI Appendix, Fig. S5D*), as well as a rapid increase in MRAP, Nur77, and CYP11A1 hnRNA and mRNA. Unexpectedly, we observed a decrease in MC2R hnRNA and mRNA, and small dynamic changes were also observed for HSL hnRNA and mRNA (*SI Appendix, Fig. S5E*). In contrast, there was no effect on CYP11A1 and HSL protein (*SI Appendix, Fig. S5F*).

Overall, there was a good qualitative fit between our model predictions and our experimental data for both small and large

ACTH perturbations (Figs. 2 and 3, respectively). Importantly, the network architecture and parameter values in our SRN model were identical in both cases. This suggests that, for the majority of the molecular species considered in the model, no new mechanisms controlling the SRN dynamic response have to be introduced to explain the dynamic SRN responses to ACTH stimuli of varying magnitude.

Dynamic Responses of the SRN to an LPS Challenge. Our mathematical model of the SRN suggests that the adrenal response to ACTH is primarily dependent on the specific pattern of ACTH stimulation. However, in several stress scenarios, the adrenal can be influenced by other additional factors that modulate the SRN response. For example, activation of the immune system by administration of the bacterial endotoxin LPS is known to induce CORT secretion through a robust activation of the HPA axis, as well as through a direct effect at the level of adrenocortical steroidogenic cells (33). Therefore, we investigated the dynamic pattern of adrenal activation in response to such a stimulus. As previously shown (8), LPS administration induced an elevated and prolonged ACTH response (Fig. 4A) that was followed by a long-lasting A-CORT (Fig. 4B) and P-CORT (*SI Appendix, Fig. S6B*) response. Unexpectedly, despite the high levels of A-CORT measured after the LPS injection, there was no significant effect of LPS on pGR (Fig. 4C). An elevated and long-lasting effect of

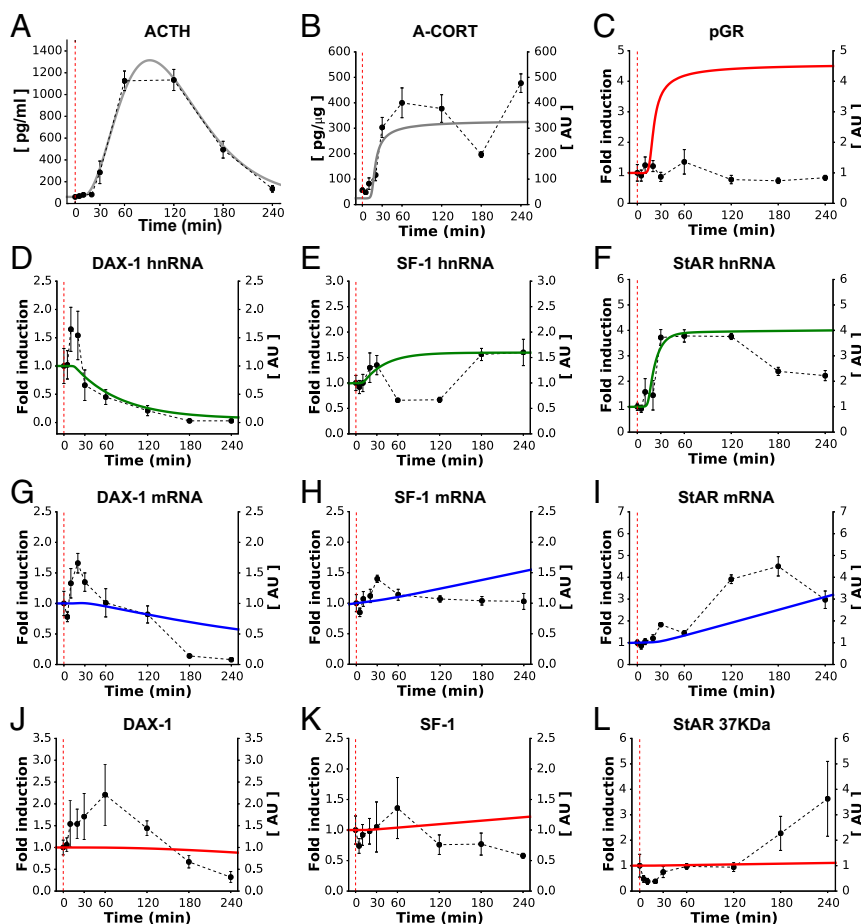


Fig. 4. Before considering the cross-talk with the immune pathway, the model partially reproduced the dynamic effects of an LPS-induced pulse of ACTH (A) on components of the SRN. Although it ignores cytokine effects, the model successfully reproduced the long and sustained surge of A-CORT (B), but not of GR activation (C). The model also made qualitative predictions about the gene expression dynamics that closely matched the DAX-1 *in vivo* data (D, G, and J), but failed to reproduce the SF-1 (E, H, and K) and StAR (F, I, and L) gene expression dynamics. Red dashed lines indicate the time of LPS injection. Representative Western immunoblotting images for pGR, StArp37, SF-1, and DAX-1 are shown in *SI Appendix, Fig. S6*.

LPS was observed on the genomic adrenal steroidogenic pathway, including StAR hnRNA and mRNA (Fig. 4 *F* and *I*), and a multiphasic effect on SF-1 hnRNA (Fig. 4*E*) with a small non-significant increase in SF-1 mRNA (Fig. 4*H*). In contrast to the decrease in DAX-1 observed in the high-ACTH dose experiment, we observed a biphasic dynamic effect on DAX-1 hnRNA and mRNA (Fig. 4 *D* and *G*). We also measured the effects of LPS on protein levels and found that it increased the levels of StArp37 (Fig. 4*L*) and StArp32 (SI Appendix, Fig. S6*F*), and caused a nonsignificant increase in StArp30 (SI Appendix, Fig. S6*F*). There was no effect of LPS on SF-1 protein (Fig. 4*K*), but we observed a biphasic effect of LPS on DAX-1 protein (Fig. 4*J*) that was consistent with DAX-1 hnRNA and mRNA.

In parallel to the effect on CORT, there was a robust and prolonged effect on pHSL-(Ser660) and pHSL-(Ser563), as well as dynamic changes in pCREB (SI Appendix, Fig. S6 *C* and *D*). Consistent with the findings from the high-ACTH dose experiment, LPS induced dynamic changes in MRAP, Nur77, and CYP11A1 hnRNA and mRNA and a significant decrease in MC2R and HSL hnRNA and mRNA (SI Appendix, Fig. S6*E*). Despite its effects on transcription, there was no effect of LPS on CYP11A1 and HSL protein (SI Appendix, Fig. S6*F*).

Injection of LPS in the rat is also known to increase plasma cytokines in a time-dependent manner (34). In addition, because LPS can also increase intra-adrenal expression of cytokines, we investigated the dynamics of intra-adrenal cytokines in LPS-treated rats. As expected, LPS induced a rapid and transient increase in IL-1 β hnRNA and mRNA, IL-6 hnRNA and mRNA, and TNF- α hnRNA and mRNA (SI Appendix, Fig. S7 *A–C*).

Although LPS increases both ACTH and cytokine levels, it is not clear whether these cytokines modulate the SRN response to ACTH and the mechanisms through which this may occur. To investigate this, we drove our model of the SRN with the ACTH pattern generated by the LPS injection and compared its output with the experimental data (Fig. 4*A*). Our model roughly approximated the dynamics of A-CORT and the DAX-1 hnRNA (Fig. 4 *B* and *D*). In contrast, the expression dynamics of SF-1 and StAR showed some discrepancies in their hnRNA dynamics (Fig. 4 *E* and *F*), where the model failed to reproduce the biphasic induction of these genes. Parallel to A-CORT, the model predicted induction and sustained activation of pGR. This was in stark contrast with our experimental data showing a lack of pGR activation despite high A-CORT (Fig. 4*C*). Taken together, these results suggest that a model of the SRN lacking cytokine regulation is not sufficient to explain its response to LPS.

Dynamic Effects of LPS-Induced Adrenal Cytokine Expression on the SRN. The lack of GR activation in response to LPS, together with the fact that LPS has been shown to repress GR function in other tissues (reviewed in ref. 35), points to an interaction between cytokines and GR. Indeed, previous findings show that the LPS-induced proinflammatory cytokine TNF- α inhibits GR phosphorylation in Serine 211 in human airway cells (36). In light of this, we extended our model to account for cross-talk between components of the SRN and the immune pathway, and used it to test whether these interactions could account for the observed response to LPS. To do this, we constructed a map of the network architecture to elucidate its effects upon steroidogenesis (SI Appendix, Fig. S8 and *Mathematical Model*). As was the case for the full steroidogenic network, we simplified the map of interactions between the immune pathway and the SRN (Fig. 5 and SI Appendix, *Mathematical Model*). Furthermore, our time-course data on cytokine mRNA levels measured in the adrenals exhibited a timescale similar to cytokine protein dynamics in plasma following LPS stimulation (34). Thus, we accounted for the effects that cytokines TNF- α , IL-1 β , and IL-6 have upon specific components of the SRN by using their mRNA time-course data. In other words, in addition to the high-ACTH

response elicited by LPS, we used the cytokines' dynamic profiles as additional, selective input to specific targets within the SRN (SI Appendix, Fig. S9).

We modified the mathematical model to account for these cytokine effects (SI Appendix, *Mathematical Model*) and carried out computer simulations to explore the steroidogenic response to LPS. The mathematical model predicted not only the sustained induction of A-CORT (Fig. 6*B*), but also the inhibition of pGR that was observed following LPS injection (Fig. 6*C*; compare with Fig. 4*C*). The model also predicted the transient, multiphasic induction of SF-1 and StAR genes (Fig. 6 *E* and *F*) as well as the transient inhibition of DAX-1 gene expression (Fig. 6*D*) and SF-1, StAR, and DAX-1 mRNA and protein dynamics (Fig. 6 *G–L*).

Discussion

Previous studies of adrenal steroidogenesis have focused on specific interactions between genes and proteins involved in glucocorticoid synthesis. Although these studies have provided important biological insight into the structure and regulation of key steroidogenic factors, the dynamics of the interactions of these factors across different timescales has not been considered. Indeed, using static data on individual interactions within the steroidogenic pathway has not been sufficient to explain how specific patterns of ACTH stimulation are translated by the adrenals into specific patterns of CORT secretion.

To understand this, we explored how some of these factors interact with one another in the context of a complex dynamic regulatory network. Because of the dynamic nature of steroidogenesis, we developed a mathematical model of the SRN that accounted for regulatory processes occurring at different timescales. Importantly, we also considered an intra-adrenal CORT-mediated feedback loop, the effects of which were previously described through mathematical modeling (17). We used our model to predict the time evolution of steroidogenesis following a series of physiological perturbations relevant to stress and inflammation. By testing these predictions experimentally, we have shown how the SRN can respond to both small and large ACTH perturbations and how the coupling with the immune pathway may be necessary to elicit an ACTH/CORT-dissociated response during inflammation.

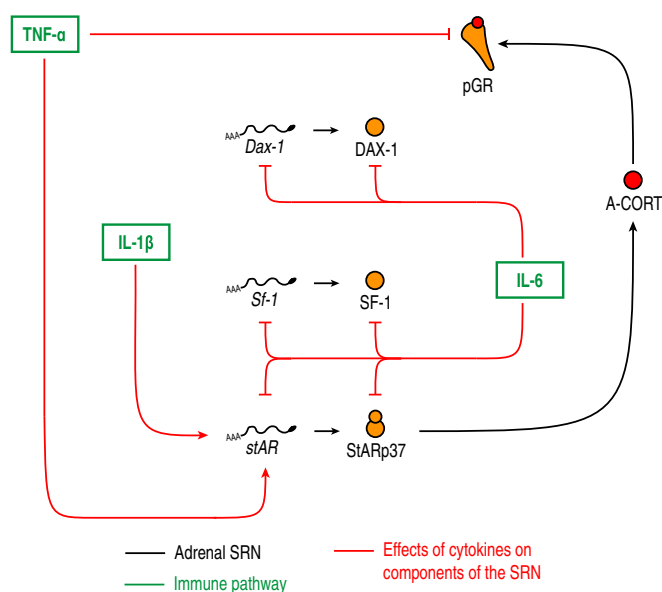


Fig. 5. Cytokine effects upon targets within the adrenal SRN considered in the model. The transient cytokine pulses elicited by LPS were used as additional input functions to ACTH.

hypothesize that mechanisms such as these could explain the discrepancies we have observed.

Recent data from our group suggest that, in addition to the well-known CORT-mediated negative feedback at the pituitary and brain regulating HPA axis activity, an intra-adrenal negative feedback involving activation of the GR can rapidly inhibit ACTH-induced glucocorticoid synthesis (17). Consistent with this, there is evidence that glucocorticoids can inhibit the transcription of steroidogenic genes through a mechanism that involves the synergistic association of SF-1 and GR to modulate DAX-1 expression (20). The present study provides further evidence to support this hypothesis by showing that a rapid, transient activation of adrenal GR tightly follows the dynamics of intra-adrenal corticosterone.

Further implications of an intra-adrenal CORT negative feedback loop relate to the role that the DAX-1, SF-1, and StAR genes play in controlling CORT synthesis. For example, although DAX-1 expression is critical for normal HPA organ development (40–42), its role in regulating steroidogenesis in the adult is still unclear. SF-1 and GR have been shown to synergistically modulate DAX-1 expression (20), which in turn inhibits SF-1-mediated induction of StAR (43). ACTH is known to disrupt this SF-1/GR synergistic effect on DAX-1 (20), and GR is activated by intra-adrenal CORT. This suggests that DAX-1 may be acting as an organizing “hub” by simultaneously integrating and decoding hormone signals from both the pituitary and the adrenal to control steroidogenesis. If this is the case, it is possible that changes in the way this “hub” functions could lead to alterations in the way the adrenal SRN responds to ACTH perturbations.

We also studied the steroidogenic response to an LPS injection. In this case, not only the SRN but also the immune pathway was activated, as shown by the induction of cytokines TNF- α , IL-6, and IL-1 β . The cross-talk between the steroidogenic and immune pathways has been modeled previously, although only at the system level (37). The mathematical model that we present here is the first to incorporate a detailed description of the SRN and its interactions with the immune pathway. Notably, our model failed to reproduce the LPS response until we explicitly accounted for the effects that cytokines have upon specific components within the SRN. This suggests that cytokines interact with ACTH to mediate the inflammatory response at the level of the adrenal SRN. Although it has been shown that a severe stressor can increase cytokine levels in the brain and pituitary even in the absence of inflammation (44), and that ACTH can increase cytokine secretion in the adrenal gland *in vitro* (45, 46), we did not see such an increase in the level of adrenal cytokines following a high-ACTH stimulation alone.

A surprising finding of our study is the biphasic change in DAX-1 hnRNA, mRNA, and protein observed in the LPS experiment. Although it is known that IL-6 down-regulates DAX-1 gene expression in bovine zona fasciculata cells (47), studies in different steroidogenic tissues have shown that TNF- α can increase the expression of DAX-1 protein (48). Indeed, a rapid increase in TNF- α levels in plasma has been observed shortly after LPS stimulation in the rat (34), and we have observed a rapid increase in TNF- α hnRNA and mRNA in this study. It is therefore tempting to speculate that a transient enhancement of DAX-1 in response to increased TNF- α may occur in the zona fasciculata of rats injected with LPS before the decrease induced by IL-6.

The sustained CORT response to transient ACTH following an LPS injection suggests a disruption in the GR-mediated intra-adrenal feedback loop. This could be a factor underlying the dissociated dynamics between ACTH and CORT observed in stress scenarios. Uncovering the origin of these dissociated dynamics is key to understanding a number of physiological and pathological conditions where sustained high levels of CORT have been observed even after ACTH has returned to normal (8). Consistent with this, our model predicts that cytokine effects on

the DAX-1 regulatory “hub” of the SRN may explain the dynamic dissociation between ACTH and CORT during inflammation.

With regard to other measured factors that were not included in the model, on the whole, we observed a dynamic activity that was consistent with the ACTH and/or LPS stimulation. However, we did note some discrepancies with previous studies; for example, it has been shown that ACTH induces the expression of MC2R (25). However, in our study we found that, although a small pulse of ACTH increased MC2R hnRNA and mRNA, administration of LPS decreased MC2R hnRNA and mRNA. Similarly, although a pulse of ACTH had no effect on HSL expression, LPS decreased both HSL hnRNA and mRNA. This suggests that inflammatory stress can lead to a decrease in ACTH signaling and cholesterol availability, which may in turn lead to adrenal hypo-responsiveness in the longer-term that is often observed in chronic inflammation and sepsis (49).

In summary, we have presented a mathematical model of steroidogenesis that makes qualitative predictions in response to a range of ACTH stimuli. Further *in vitro* experiments are required to shed light on the specific molecular mechanisms regulating the cross-talk between steroidogenic genes, which would enable us to refine our models to make quantitative predictions. Nonetheless, we have shown that our mathematical model of the adrenal SRN delivers valuable insight about the transient and rapid adrenal dynamics observed in response to ACTH perturbations during both basal and acute stress scenarios. In future work, the model could be further exploited to study several ACTH-independent mechanisms regulating adrenal steroidogenesis, such as modulation by the splanchnic nerve (50), the influence of metabolic factors such as leptin and insulin (6), and the effects of acute or chronic exposure to synthetic glucocorticoids.

Materials and Methods

Animals and Surgery. All experiments were conducted on adult male Sprague-Dawley rats (Harlan Laboratories) weighing 220–250 g at the time of arrival.

Rats were anesthetized using isoflurane, and an indwelling catheter was inserted in the right jugular vein as previously described (51).

Experiments and Tissue Collection. All experiments started at 9 AM and were performed 5–7 d after the surgery. Rats were given the following: (i) an i.v. injection of synthetic ACTH (10 ng/0.1 mL; ACTH pulse experiment); (ii) four s.c. injections of ACTH (2 μ g/kg; high-dose ACTH experiment); and (iii) an i.v. injection of LPS (25 μ g per rat in 0.1 mL of sterile saline; LPS experiment).

After decapitation, trunk blood was collected and plasma processed for ACTH and corticosterone measurement as previously described (51). Adrenal glands were collected and the inner zones (comprising the zona fasciculata and the zona reticularis of the cortex and the adrenal medulla) were separated from the outer zone (containing the zona glomerulosa and the capsula). Individual inner zones were immediately frozen until processing for isolation of RNA for real-time quantitative PCR (left adrenal) and for protein extraction for Western immunoblotting and corticosterone measurement (right adrenal) as previously described (38, 52).

Statistical Analysis. Data were analyzed using the nonparametric Kruskal-Wallis Test. Statistical significance was set at $P < 0.05$.

Mathematical Model. We developed a mathematical model of the adrenal SRN that accounts for the time evolution of core components of the full network, namely A-CORT, pGR, and the genes DAX-1, SF-1, and StAR. The model postulates a network architecture based on known biological interactions with parameter values estimated from the literature and calibrated using the ACTH i.v. pulse data. The network architecture and kinetic parameter values remained invariant for generating predictions about the high s.c. ACTH and LPS challenge experiments.

Because of the involvement of a slow genomic pathway and a fast non-genomic one, we wrote the model in terms of a set of DDEs, where the delays were associated with the gene transcription and translation processes. Our set of nonlinear, coupled DDEs was numerically integrated using XPPAUT (53) and PyDDE with a fixed-time step of 0.001 min and a fourth-order Runge–Kutta

integrator with adaptive steps. The model development and complete set of model equations are detailed in *SI Appendix, Mathematical Model*.

More details on materials and methods can be found in *SI Appendix, Supplementary Materials and Methods*. Access to data, associated protocols, code, and materials is available upon reasonable request.

- Ixart G, et al. (1994) Short-term but not long-term adrenalectomy modulates amplitude and frequency of the CRH41 episodic release in push-pull cannulated median eminence of free-moving rats. *Brain Res* 658:185–191.
- Ixart G, Barbanel G, Nougouier-Soulé J, Assenmacher I (1991) A quantitative study of the pulsatile parameters of CRH-41 secretion in unanesthetized free-moving rats. *Exp Brain Res* 87:153–158.
- Walker JJ, et al. (2012) The origin of glucocorticoid hormone oscillations. *PLoS Biol* 10: e1001341.
- Walker JJ, Terry JR, Lightman SL (2010) Origin of ultradian pulsatility in the hypothalamic-pituitary-adrenal axis. *Proc Biol Sci* 277:1627–1633.
- Henley DE, et al. (2009) Development of an automated blood sampling system for use in humans. *J Med Eng Technol* 33:199–208.
- Bornstein SR, Engeland WC, Ehrhart-Bornstein M, Herman JP (2008) Dissociation of ACTH and glucocorticoids. *Trends Endocrinol Metab* 19:175–180.
- Tkachenko IV, Jääskeläinen T, Jääskeläinen J, Palvimo JJ, Voutilainen R (2011) Interleukins 1 α and 1 β as regulators of steroidogenesis in human NCI-H295R adrenocortical cells. *Steroids* 76:1103–1115.
- Gibbison B, et al. (2015) Dynamic pituitary-adrenal interactions in response to cardiac surgery. *Crit Care Med* 43:791–800.
- Kraemer FB, Shen WJ (2002) Hormone-sensitive lipase: Control of intracellular tri-(di-)acylglycerol and cholesteryl ester hydrolysis. *J Lipid Res* 43:1585–1594.
- Lin D, et al. (1995) Role of steroidogenic acute regulatory protein in adrenal and gonadal steroidogenesis. *Science* 267:1828–1831.
- Caron KM, et al. (1997) Characterization of the promoter region of the mouse gene encoding the steroidogenic acute regulatory protein. *Mol Endocrinol* 11:138–147.
- Martin LJ, Boucher N, Brousseau C, Tremblay JJ (2008) The orphan nuclear receptor NUR77 regulates hormone-induced STAR transcription in Leydig cells through co-operation with Ca²⁺/calmodulin-dependent protein kinase I. *Mol Endocrinol* 22: 2021–2037.
- Jo Y, Stocco DM (2004) Regulation of steroidogenesis and steroidogenic acute regulatory protein in R2C cells by DAX-1 (dosage-sensitive sex reversal, adrenal hypoplasia congenita, critical region on the X chromosome, gene-1). *Endocrinology* 145:5629–5637.
- Carsia RV, Malamed S (1979) Acute self-suppression of corticosteroidogenesis in isolated adrenocortical cells. *Endocrinology* 105:911–914.
- Loose DS, Do YS, Chen TL, Feldman D (1980) Demonstration of glucocorticoid receptors in the adrenal cortex: Evidence for a direct dexamethasone suppressive effect on the rat adrenal gland. *Endocrinology* 107:137–146.
- Peron FG, Moncloa F, Dorfman RI (1960) Studies on the possible inhibitory effect of corticosterone on corticosteroidogenesis at the adrenal level in the rat. *Endocrinology* 67:379–388.
- Walker JJ, et al. (2015) Rapid intra-adrenal feedback regulation of glucocorticoid synthesis. *JR Soc Interface* 12:20140875.
- Briassoulis G, Damjanovic S, Xekouki P, Lefebvre H, Stratakis CA (2011) The glucocorticoid receptor and its expression in the anterior pituitary and the adrenal cortex: A source of variation in hypothalamic-pituitary-adrenal axis function; implications for pituitary and adrenal tumors. *Endocr Pract* 17:941–948.
- Chong C, et al. (2017) Regulation of aldosterone secretion by mineralocorticoid receptor-mediated signaling. *J Endocrinol* 232:525–534.
- Gummow BM, Scheys JO, Cancelli VR, Hammer GD (2006) Reciprocal regulation of a glucocorticoid receptor-steroidogenic factor-1 transcription complex on the Dax-1 promoter by glucocorticoids and adrenocorticotropin hormone in the adrenal cortex. *Mol Endocrinol* 20:2711–2723.
- Babu PS, et al. (2002) Interaction between Dax-1 and steroidogenic factor-1 in vivo: Increased adrenal responsiveness to ACTH in the absence of Dax-1. *Endocrinology* 143:665–673.
- Fan W, et al. (2004) Protein kinase A potentiates adrenal 4 binding protein/steroidogenic factor 1 transactivation by reintegrating the subcellular dynamic interactions of the nuclear receptor with its cofactors, general control nonderepressed-5/transformation/transcription domain-associated protein, and suppressor, dosage-sensitive sex reversal-1: A laser confocal imaging study in living KGN cells. *Mol Endocrinol* 18:127–141.
- Sugawara T, et al. (1997) Regulation of expression of the steroidogenic acute regulatory protein (STAR) gene: A central role for steroidogenic factor 1. *Steroids* 62:5–9.
- Sugawara T, Kiriakidou M, McAllister JM, Kallen CB, Strauss JF, III (1997) Multiple steroidogenic factor 1 binding elements in the human steroidogenic acute regulatory protein gene 5'-flanking region are required for maximal promoter activity and cyclic AMP responsiveness. *Biochemistry* 36:7249–7255.
- Winnay JN, Hammer GD (2006) Adrenocorticotropin hormone-mediated signaling cascades coordinate a cyclic pattern of steroidogenic factor 1-dependent transcriptional activation. *Mol Endocrinol* 20:147–166.
- Carnes M, Brownfield MS, Kalin NH, Lent S, Barksdale CM (1986) Episodic secretion of ACTH in rats. *Peptides* 7:219–223.
- Carnes M, Kalin NH, Lent SJ, Barksdale CM, Brownfield MS (1988) Pulsatile ACTH secretion: Variation with time of day and relationship to cortisol. *Peptides* 9:325–331.
- Wang Z, Frederick J, Garabedian MJ (2002) Deciphering the phosphorylation “code” of the glucocorticoid receptor in vivo. *J Biol Chem* 277:26573–26580.
- Liu Y, et al. (2013) Transcriptional regulation of episodic glucocorticoid secretion. *Mol Cell Endocrinol* 371:62–70.
- Spiga F, Liu Y, Aguilera G, Lightman SL (2011) Temporal effect of adrenocorticotropin hormone on adrenal glucocorticoid steroidogenesis: Involvement of the transducer of regulated cyclic AMP-response element-binding protein activity. *J Neuroendocrinol* 23: 136–142.
- Anthonsen MW, Rönstrand L, Werndt C, Degerman E, Holm C (1998) Identification of novel phosphorylation sites in hormone-sensitive lipase that are phosphorylated in response to isoproterenol and govern activation properties in vitro. *J Biol Chem* 273:215–221.
- Ragazzon B, et al. (2006) Adrenocorticotropin-dependent changes in SF-1/DAX-1 ratio influence steroidogenic genes expression in a novel model of glucocorticoid-producing adrenocortical cell lines derived from targeted tumorigenesis. *Endocrinology* 147:1805–1818.
- Zacharowski K, et al. (2006) Toll-like receptor 4 plays a crucial role in the immune-adrenal response to systemic inflammatory response syndrome. *Proc Natl Acad Sci USA* 103:6392–6397.
- Givalois L, et al. (1994) Temporal cascade of plasma level surges in ACTH, corticosterone, and cytokines in endotoxin-challenged rats. *Am J Physiol* 267:R164–R170.
- Marketon JI, Sternberg EM (2010) The glucocorticoid receptor: A revisited target for toxins. *Toxins (Basel)* 2:1357–1380.
- Bouazza B, et al. (2012) Cytokines alter glucocorticoid receptor phosphorylation in airway cells: Role of phosphatases. *Am J Respir Cell Mol Biol* 47:464–473.
- Malek H, Ebadzadeh MM, Safabakhsh R, Razavi A, Zaringhalam J (2015) Dynamics of the HPA axis and inflammatory cytokines: Insights from mathematical modeling. *Comput Biol Med* 67:1–12.
- Spiga F, et al. (2011) ACTH-dependent ultradian rhythm of corticosterone secretion. *Endocrinology* 152:1448–1457.
- Desroches-Castan A, Feige JJ, Cherradi N (2017) ACTH action on messenger RNA stability mechanisms. *Front Endocrinol (Lausanne)* 8:3.
- Achermann JC, Meeks JJ, Jameson JL (2001) Phenotypic spectrum of mutations in DAX-1 and SF-1. *Mol Cell Endocrinol* 185:17–25.
- Iyer AK, McCabe ER (2004) Molecular mechanisms of DAX1 action. *Mol Genet Metab* 83:60–73.
- Zhao Y, et al. (2006) Zebrafish dax1 is required for development of the interrenal organ, the adrenal cortex equivalent. *Mol Endocrinol* 20:2630–2640.
- Zazopoulos E, Lalli E, Stocco DM, Sassone-Corsi P (1997) DNA binding and transcriptional repression by DAX-1 blocks steroidogenesis. *Nature* 390:311–315.
- Connor KA, et al. (2003) Inescapable shock induces resistance to the effects of dexamethasone. *Psychoneuroendocrinology* 28:481–500.
- Judd AM, MacLeod RM (1992) Adrenocorticotropin increases interleukin-6 release from rat adrenal zona glomerulosa cells. *Endocrinology* 130:1245–1254.
- Call GB, et al. (2000) Bovine adrenal cells secrete interleukin-6 and tumor necrosis factor in vitro. *Gen Comp Endocrinol* 118:249–261.
- Mclmloil S, Strickland J, Judd AM (2016) Interleukin 6 increases the in vitro expression of key proteins associated with steroidogenesis in the bovine adrenal zona fasciculata. *Domest Anim Endocrinol* 55:11–24.
- Sadasivam M, Ramachandirin B, Balakrishnan S, Prahathan C (2015) Tnf- α -mediated suppression of Leydig cell steroidogenesis involves DAX-1. *Inflammation Research* 64: 549–556.
- Boonen E, Bornstein SR, Van den Bergh G (2015) New insights into the controversy of adrenal function during critical illness. *Lancet Diabetes Endocrinol* 3:805–815.
- Ulrich-Lai YM, Arnholt MM, Engeland WC (2006) Adrenal splanchnic innervation contributes to the diurnal rhythm of plasma corticosterone in rats by modulating adrenal sensitivity to ACTH. *Am J Physiol Regul Integr Comp Physiol* 290:R1128–R1135.
- Spiga F, et al. (2007) Effect of the glucocorticoid receptor antagonist Org 34850 on basal and stress-induced corticosterone secretion. *J Neuroendocrinol* 19:891–900.
- Park SY, et al. (2013) Constant light disrupts the circadian rhythm of steroidogenic proteins in the rat adrenal gland. *Mol Cell Endocrinol* 371:114–123.
- Ermentrout B (2007) *Simulating, Analyzing, and Animating Dynamical Systems: A Guide to XPPAUT for Researchers and Students* (Siam, Philadelphia).